*J. Physiol.* (1977), **265**, *pp.* 721–741
*With 9 text-figures*
*Printed in Great Britain*



# BACKGROUND ADAPTATION IN THE RODS OF THE FROG'S RETINA

BY SIMO HEMILÄ

*From the Department of Zoology, University of Helsinki, Helsinki 10, Finland*

(*Received 28 June 1976*)

SUMMARY

1. Aspartate-isolated photoresponses of the red rods to flashes and steps of light have been recorded, both in the presence of and without background lights of varying strength.

2. The results are interpreted in terms of a model of rod outer segment adaptation, where the three model parameters correspond to the adaptation processes associated with the transmitter release, the transmitter background concentration and the plasma membrane leakage, respectively.

3. The stimulus–response function deviated somewhat from the Michaelis equation $U/U_{max} = I/(I + I_H)$. During light-adaptation the operating curve, the stimulus–response function plotted in a log–log diagram, retained approximately its shape while moving strongly to the right along the log intensity axis and to a lesser degree downwards ($U_{max}$-decrease).

4. The movement of the operating curve was such that the rods approximately obeyed Weber's law. In the cases of flash and step of light stimuli the movement of the operating curve was about the same.

5. When a moderate background light was turned on a large decrease of sensitivity was first observed. During a period 0·5–1 min the sensitivity increased towards the stationary value. After extinguishing the background light the dark sensitivity returned in 0·5–1 min and then a period of hypersensitivity lasting typically 1 min was observed.

6. The experimental results, as interpreted according to the model, indicate that light-adaptation decreases $q$, the number of transmitter molecules released by one bleached rhodopsin molecule.

7. There is probably an adaptation process also in the rod inner segment, which increases the sensitivity of the rod to transient stimuli.

## INTRODUCTION

Background adaptation here signifies the fast adaptation processes in the retina when a weak or moderate background light is turned *on*

(light-adaptation) or *off* (fast dark-adaptation). The background exposures are supposed to be 'non-bleaching', bleaching say less than 1% of rhodopsin during the time they were applied. Background adaptation occurs at the receptor level (receptor adaptation) and in the neuronal network of the retina (network adaptation). In this work the background adaptation processes in the red rods of the frog retina are studied.

Receptor potentials can be recorded intracellularly, extra-cellularly with fractional depth techniques, or across the whole retina when the electroretinogram (e.r.g.)-components of non-receptor origin are eliminated. In this work the receptor potential (distal P III) was isolated with aspartate, which eliminates the P II component of the e.r.g. (Furukawa & Hanawa, 1955). There occurs also a proximal P III component of non-receptor origin (Murakami & Kaneko, 1966). According to Sillman, Ito & Tomita (1969) aspartate eliminates even this component in the frog and gives receptor potentials similar to those observed by fractional depth techniques.

The receptor potential as a function of the stimulus light intensity, plotted on the log.–log. diagram, is here termed *operating curve*. The adaptation processes do not change the shape of the operating curve appreciably but move the curve along the axes. The first aim of this work was to determine the frog rod operating curves both in stationary states at different background intensities and also during the periods after a chosen background light was turned *on* or *off* to observe the transient changes. The second aim was to compare the experimental results with a model of rod outer segment adaptation. That model predicts certain displacements of the operating curve caused by adaptation mechanisms in the rod outer segment, and thus comparison with the model can help us to point out certain possible adaptation mechanisms and exclude others. A detailed description of the model will be published elsewhere.

## THEORY

### *The model of rod outer segment adaptation*

*Definitions*

| | |
|---|---|
| $B$ | the fraction of sodium channels closed |
| $c$ | the transmitter concentration in the rod outer segment |
| $c_1$ | the transmitter background, the initial transmitter concentration before stimulation |
| $c_H$ | the transmitter concentration corresponding to $B = 1/2$ |
| $c_1$, $c_2$ | the parameters of the general photoresponse equations (eqn. (5)) |
| $c_0$ | $= c_H(1 + R_s G_0)$ |
| $E$ | the source voltage (e.m.f.) in the rod inner segment |
| $G_0$ | the number of sodium channels multiplied by the conductance of one channel |

$G_p$ = $G_o(1-B)$, the total conductance of the open channels
$G_L$ the leakage conductance of the outer segment plasma membrane
$I$ the stimulus intensity
$I_H$ the stimulus intensity which elicits a response $\frac{1}{2}U_{max}$
$I_h$ the value of $I_H$ in the dark-adapted state
$I_t$ the threshold intensity corresponding to the criterion response $U_c$
$I_o$ the absolute threshold intensity (dark-adapted state)
$I_B$ the background light intensity
$I_{B\,rel}$ the relative background light intensity ($I_{B\,rel} = 1$ corresponds to the bleaching rate $3 \times 10^{-10}$ sec$^{-1}$)
$I_D$, $\beta$ the constants used in the fitting of a generalized Weber's function
$Q$ the transmitter coefficient: $c = c_1 + QI$
$Q_o$ the value of $Q$ in the dark-adapted state
$Q^*$ = $Q/\tau_i$
$q$ the transmitter release factor, the average number of transmitter molecules liberated by an isomerizing quantum
$R_e$ the resistance of the intercellular space (Fig. 1)
$R_i$ the resistance of the inner segment plasma membrane
$R_c$ the resistance of the cilium
$R_s$ = $R_e + R_i + R_c$
$U$ the receptor potential, the change in voltage across the resistance $R_s$ brought about by the stimulus light
$U_{max}$ the maximum receptor potential in the prevailing state of adaptation
$U_m$ the value of $U_{max}$ in the dark-adapted state
$U_c$ the criterion photoresponse in threshold measurements
$\tau$ the average life time of the transmitter molecules
$\tau_i$ the integrating time in the response to the step of light

Fig. 1 shows the electric network of the rod assumed in the model. The sodium channel conductance $G_p$ and the leakage conductance $G_L$ are both affected (though not equally) by the adapting light. The basic assumptions are conventional: light liberates from the disks internal transmitter molecules, which close $Na^+$-channels in the plasma membrane of the rod outer segment. The transmitter background $c_1$ is the initial concentration of transmitter (assumed to be negligible in the dark-adapted state). A step of light intensity $I$ causes a fast increase $QI$ of the transmitter concentration:

$$c = c_1 + QI. \tag{1}$$

*The transmitter coefficient* $Q$ is proportional to *the transmitter release factor* $q$, the average number of transmitter molecules (possibly $Ca^{2+}$) liberated by an isomerizing quantum and to *the average life time* $\tau$ of the transmitter molecules before they are reabsorbed or otherwise inactivated. Both $q$ and $\tau$ may depend on the adaptational state of the rod outer segment. In dark-adapted state $Q = Q_o$.

When stimulating by a step of light the coefficient $Q$ is proportional to an integrating time: $Q = Q^* \tau_i$ (see Baylor, Hodgkin & Lamb, 1974).

Eqn. (1) also holds for flash stimuli, because in that case the transient increase of the transmitter concentration is proportional to the flash intensity $I$ and to the duration of the flash, $\Delta t$. Therefore, $Q = Q^* \Delta t$.

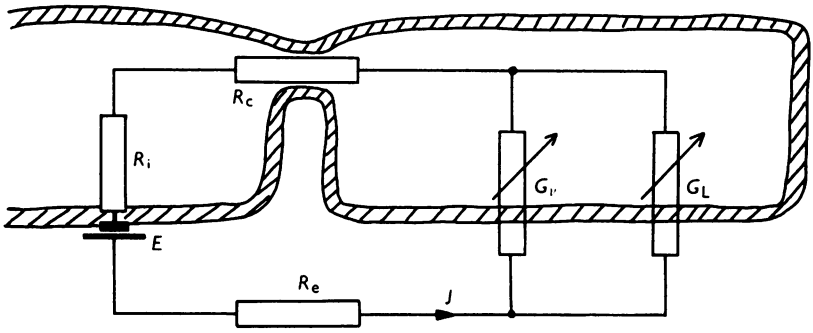


Fig. 1. The equivalent circuit of the rod. $R_i$ is the resistance of the inner segment plasma membrane, $R_c$ is the resistance of the cilium, $R_e$ is the small resistance of the intercellular space. $G_v$ is the conductance of the $Na^+$ channels and $G_L$ is the leakage conductance. $E$ is the source voltage (e.m.f.) caused by the sodium pump.

The total conductance of all the sodium channels in the plasma membrane of the rod outer segment is denoted $G_0$. The transmitter molecules are assumed to bind rapidly and reversibly to the channels, closing a fraction $B$ of these channels. The closing rate of the channels is proportional to the product $(1-B)c$, the opening rate is proportional to $B$. In equilibrium these rates are equal and thus $B = c/(c+c_H)$, where $c_H$ is a constant (the concentration corresponding to $B = 1/2$). The channel conductance is then

$$G_v = G_0(1-B) = G_0/(1+c/c_H). \tag{2}$$

The stimulation $I$ increases $c$ (eqn. (1)) and thus decreases $G_v$ (eqn. (2)), eliciting a 'receptor potential' $U$, a decrease in voltage across the resistance $R_e$ in Fig. 1. An upper limit of this photoresponse, $U_m$, is reached when the dark-adapted receptor ($Q = Q_0$, $c_1 = 0$) is stimulated by a high intensity ($I \to \infty$). The relative photoresponse, obtained by trivial but tedious algebraic reductions, is then

$$\frac{U}{U_m} = \frac{U_{max}}{U_m} \cdot \frac{I}{I+I_H}, \tag{3}$$

$$I_H = \frac{c_1+c_l}{Q}, \quad \frac{U_m}{U_{max}} = \frac{c_1+c_l}{c_2}, \tag{4}$$

$$c_1 = c_H\left(1+\frac{R_S G_0}{1+R_S G_L}\right), \quad c_2 = c_H \frac{1+R_S G_0}{(1+R_S G_L)^2}. \tag{5}$$

In the case of no leakage, $G_L = 0$, the parameters $c_1$ and $c_2$ are equal constants denoted $c_0$ and simpler expressions are obtained,

$$I_H = \frac{c_0 + c_1}{Q}, \quad \frac{U_m}{U_{max}} = \frac{c_0 + c_1}{c_0}, \tag{6}$$

$$c_0 = c_H(1 + R_s G_0).$$

The value of $I_H$ in the dark-adapted rod ($Q = Q_0$, $c_1 = 0$) is $I_h = c_0/Q_0$. Let $U_c$ be a small chosen criterion response in threshold measurements and let $I_t$ be the corresponding threshold intensity of the stimulating light. The absolute threshold intensity (dark-adapted rod) is denoted $I_0$. Then the log threshold increase is according to eqn. (3):

$$\log \frac{I_t}{I_0} = \underbrace{\log \frac{I_H}{I_h}}_{\text{I}} + \underbrace{\log \frac{U_m}{U_{max}}}_{\text{II}} + \underbrace{\log \frac{1 - U_c/U_m}{1 - U_c/U_{max}}}_{\text{III}}, \tag{7}$$

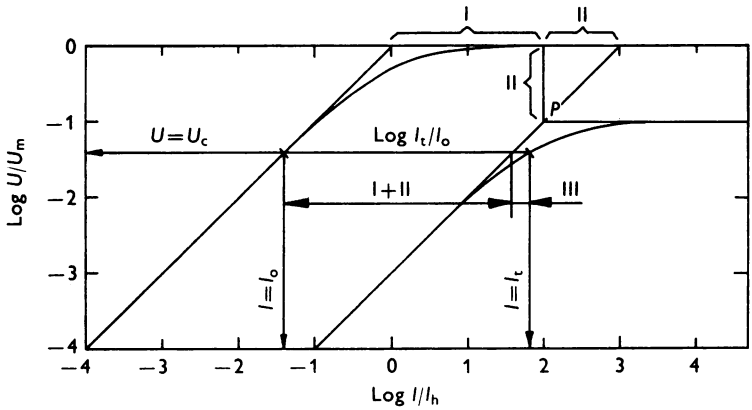


Fig. 2. Movements of the operating curve (stimulus–response curve in the log.–log. diagram): the three components of the threshold increase caused by light-adaptation. (I) a movement of the operating curve to the right; (II) a downward movement; (III) a saturating factor when $U_{max}$ approaches $U_c$. $P$ is the crossing point of the operating curve.

When the photoresponses corresponding to eqn. (3) are described by the operating curves in a log $I$, log $U$ diagram as seen in Fig. 2, the threshold $I_t$ may increase either because the increase of $I_H$ moves the curve to the right (I) or because the decrease of $U_{max}$ moves the curve downwards (II). In addition, if the decreasing amplitude $U_{max}$ approaches the chosen criterion $U_c$, the threshold increases rapidly towards infinity (III).

The predictions of the model according to eqns. (3–7) may now be summarized as follows:

(1) The operating curve, i.e. the log.–log. diagram of the stimulus–response function, retains its shape during adaptation processes. The position and the movements of the operating curve are completely described by *the crossing point P* of the extrapolated linear parts of the operating curve (co-ordinates log $I_H/I_h$, log $U_{max}/U_m$ in Fig. 2).

(2) An adapting light may change each of the parameters $Q$, $c_1$, and $G_L$, leading to characteristic movements of the operating curve.

(3) Light adaptation may decrease the transmitter coefficient $Q$ for several reasons, e.g. the adapting light may decrease the stores of the transmitter, thus reducing $q$. The decrease of $Q$ moves the operating curve an amount log $Q_o/Q$ *to the right* without reducing $U_{max}$.

(4) Any mechanism increasing the transmitter background $c_1$ moves the operating curve *down and to the right along the 45°-line*. An important such mechanism is the superposition of a background light intensity $I_B$ which creates a transmitter background $c_1 = QI_B$. The model predicts relations $U_{max} \propto I_B^{-1}$ and $I_t \propto I_B^2$ for background lights $I_B \gg I_h$ if no actual adaptation processes occur.

(5) The adapting light may also create a leakage conductance $G_L$; e.g. the bleached rhodopsin molecules in the rod outer segment plasma membrane could act as sodium leaks. The increase of $G_L$ moves the operating curve predominantly downwards but also somewhat to the left.

## METHODS

Common frogs (*Rana temporaria*) from South Finland were used throughout. They were stored at 3–4° C and kept overnight at room temperature in darkness before dissection. The retina was isolated from the excised eye under deep red light in a cooled perfusion fluid. The specimen holder consisted of a small perspex plate with a 7 mm hole, the bottom of which was covered by a meshwork of thin glass fibres. The retina was mounted receptors downwards on this meshwork and kept in place by a plastic ring (outer diameter 7 mm, inner 5 mm). The specimen holder was transferred to the perfusion chamber, where a fluid flowed past the receptor side of the retina. This fluid contained (in mM): NaCl 95; KCl 3; $CaCl_2$ 0·9; $MgCl_2$ 0·5; sodium phosphate buffer 12; glucose 10; sodium aspartate 1; and was saturated with air (the isolation of the retina had been carried out in the same fluid but containing 5 mM aspartate). Water from a thermostat pre-cooled the perfusion fluid and circulated through the water mantle of the perfusion chamber, maintaining the chosen temperature, 9 or 14° C. For details, see Donner & Hemilä (1975).

When measuring receptor potentials, the stimulating 493 nm light was either a 40 msec flash or a step of light eliciting an *on* response. The intensity of the stimulating light was varied by neutral density filters and a neutral density wedge. When measuring operating curves the time interval between successive stimulations was 2 min at 9° C and 1·5 min at 14° C. The receptor potentials were measured by two silver/silver chloride electrodes: one in the perfusion fluid below the retina and another, wire diameter 0·13 mm, just touching the upper surface of the retina (the photosensitivity of the silver chloride coating was tested; it was much too weak to affect the photoresponses of the retina). The receptor potentials were amplified

by an operational amplifier and displayed on a storage oscilloscope (Tektronix D 13) or recorded with a fast ink-jet recorder (Siemens Oscillomink).

The red background light comprised a wave-length band above 610 nm (Kodak wratten filter 29). It light-adapted the cones very efficiently, thus suppressing the cone contribution in the photoresponses of the red rods. The intensity of the background light was varied in powers of ten by neutral density filters.

The bleaching rate is a suitable quantity in describing the intensities of the stimulating and background lights. The fraction of rhodopsin bleached by the full stimulating light in a chosen period of time was measured using the spectrophotometric apparatus described in Donner & Hemilä (1975). According to this calibration the bleaching rate of the step stimulus intensity of a typical absolute threshold (criterion 12 $\mu$V) was $2 \times 10^{-10}$ sec$^{-1}$. This corresponds to bleaching in a rod 0·3 molecules per second, if a rod contains $1{\cdot}5 \times 10^{9}$ rhodopsin molecules (Donner & Reuter, 1968). Typical absolute threshold intensities of the 40 msec stimuli were two decades stronger than those with long stimuli.

The bleaching rates of the available background lights were too small to be determined in this way. They were estimated by comparing the *on* responses elicited by the background lights with the *on* responses of the known stimulus lights. The weakest background used, $\log I_{\mathrm{B\,rel}} = 0$, corresponds to the bleaching rate $3 \times 10^{-10}$ sec$^{-1}$. Thus the strongest background light, $\log I_{\mathrm{B\,rel}} = 5$, bleached *ca.* 0·2% of rhodopsin per minute.

## RESULTS

### *Photoresponses*

The photoresponses of the red rods are slow. Fig. 3A shows typical shapes of the responses to flashes in a dark-adapted retina. With increasing stimulus intensity the time-to-maximum first decreases and then increases again. The responses to saturating flashes decay very slowly. Near the rod saturation a fast new response appears. This initial peak continues to grow when the flash intensity is further increased, although the rod response is saturated. Thus this peak is mainly a cone response.

At 14° C in fresh retinae the time-to-maximum of small responses is typically 3 sec. When the flash intensity is increased, the time-to-maximum decreases to *ca.* 2 sec and then increases to *ca.* 3·5 sec when the saturation is approached. In Fig. 3*A* the time-to-maximum values are smaller (minimum *ca.* 1 sec), as is usual in somewhat older preparations. At 9° C the time-to-maximum values are 30–50% larger than at 14° C.

Fig. 3*B* shows responses to steps of light in the same dark-adapted retina (light on 8 sec). The slow rise of the response and the slow return after extinguishing the stimulus light are characteristic for the smaller responses. Again, the response becomes faster when the stimulus intensity increases. When approaching saturation, the 'off-response', the discontinuity in the slope of the potential curve, disappears. The fast initial rise is apparently caused by cones and at the highest intensity a small fast cone 'off-response' can be seen.

Fig. 3 *C* shows the effects of the background light on the time courses of the responses. The flash intensities were chosen to give approximately equal response magnitudes. Again when increasing stimulus intensity the time-to-maximum first decreases and then increases. The cone peak in the last track is somewhat more pronounced than in fresh retinae, because the cones deteriorate more slowly then the rods.

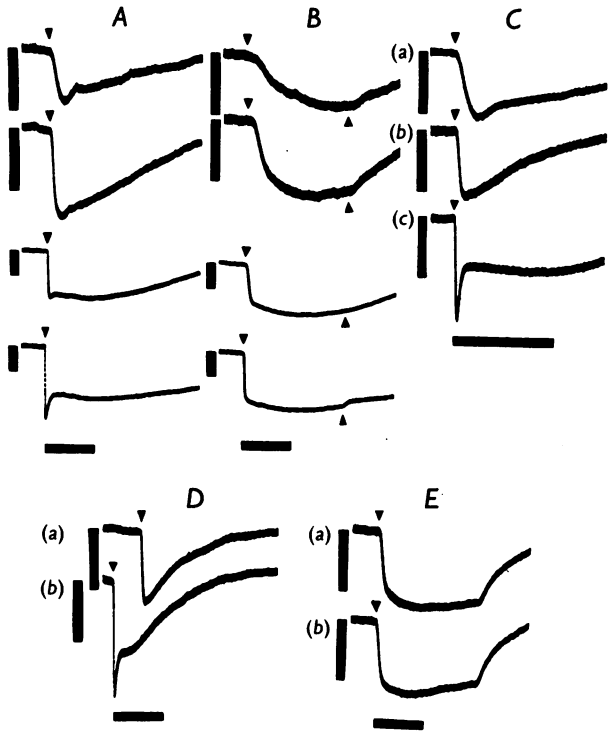


Fig. 3. Receptor potential photoresponses at 14° C. Relative intensities $I_{rel} = 1$ and $I_{B\,rel} = 1$ (log $I_{rel}$ = log $I_{B\,rel}$ = 0) correspond to the bleaching rate $3 \times 10^{-10}$ sec$^{-1}$. Scales: horizontal bars, 4 sec; vertical bars, 50 $\mu$V. *A*, dark-adapted retina, responses to 40 msec flash stimuli 493 nm, log $I_{rel}$-values 3, 3·7, 5, 6. *B*, dark-adapted retina, responses to step stimuli 493 nm, light on 8 sec, log $I_{rel}$-values 1, 1·7, 3, 4. *C*, the effect of background light on the photoresponses: flash stimuli 493 nm (note faster sweep); (*a*) in dark, log $I_{rel}$ = 3·3; (*b*) log $I_{B\,rel}$ = 2, log $I_{rel}$ = 4·5; (*c*) log $I_{B\,rel}$ = 3, log $I_{rel}$ = 6. *D*, effect of cones. Background log $I_{B\,rel}$ = 2. Flash stimuli: (*a*) 493 nm (log $I_{rel}$ = 4·4); (*b*) 568 nm. The quantum fluxes absorbed by red rods were about equal, the ratio of fluxes absorbed by cones was about ten. *E*, effect of green rods. Background log $I_{B\,rel}$ = 2. Step stimuli: (*a*) 525 nm; (*b*) 447 nm. The quantum fluxes absorbed by red rods were about equal, the ratio of the quantum fluxes absorbed by green rods was more than 50.

Although the deep red background light stimulates the cones much more strongly than the rods, the cones clearly contribute to the photoresponses near the rod saturation. The largest cone disturbance is expected in the light-adapted retina when a strong flash stimulus is applied. However, even in this situation the rod response can usually be measured with an adequate accuracy, as demonstrated in Fig. 3*D*. The 493 nm and 568 nm flashes stimulated the rods about equally (the quantum fluxes absorbed by the red rods were about the same) but the 568 nm flash stimulated the cones ten-times more than the 493 nm flash. Correspondingly a strong cone peak is observed in the lower trace. However, if the fast initial peak is omitted, the remaining responses are fairly similar and especially they have equal peak values.

The absolute threshold of green rods at 493 nm is considerably higher than that of the red rods. However, the red background light-adapts the red rods increasing their threshold but the green rods are expected to be much less light-adapted. Thus the green rods could also contribute to the photoresponses to strong stimuli in light-adapted retinae. This type of contribution to the b-wave has been observed (Frank, 1970). The interference is largest in the response to the step stimulus, because the responses of the green rods are very slow (Frank, 1970; ganglion cell measurements, Reuter & Virtanen, 1972). Thus the possible green rod contribution was tested in the light-adapted retina with 525 and 447 nm step of light stimuli. Again the red rod stimulations were about equal but the estimated green rod stimulation by the 447 nm light was nearly 2 log. units stronger than the stimulation by the 525 nm light. The recorded photoresponses in Fig. 3*E* are very nearly equal, revealing no green rod contribution. The same test was also performed using 2 log. units stronger background illumination, with the same negative result.

### *Stationary operating curves*

An operating curve obtained in the dark together with a set of stationary operating curves with relative backgrounds log $I_{\mathrm{B\,rel}} = 0$–$5$ are shown in Fig. 4. A set of operating curves of this kind was measured in nine retinae at 9° C and in four retinae at 14° C. The results can be summarized as follows.

The operating curves deviate somewhat from the curves of the model described by the Michaelis equation $U/U_{\max} = I/(I+I_{\mathrm{H}})$. Small responses are apparently proportional to the stimulus intensity but in the range $U \gtrsim 0{\cdot}1\ U_{\max}$ the curve could better be fitted with a relation

$$\frac{U}{U_{\max}} = \frac{I^n}{I^n + I_{\mathrm{H}}^n}, \quad n \approx 0{\cdot}8.$$

Thus the crossing point of the extrapolated linear parts of the operating curve (assuming that $U$ is proportional to $I$ at low intensities) does not define the curve completely, as in Fig. 2. However, adaptation does not change the shape of the operating curve appreciably and so the crossing point describes the position and the movements of the operating curve quite well.

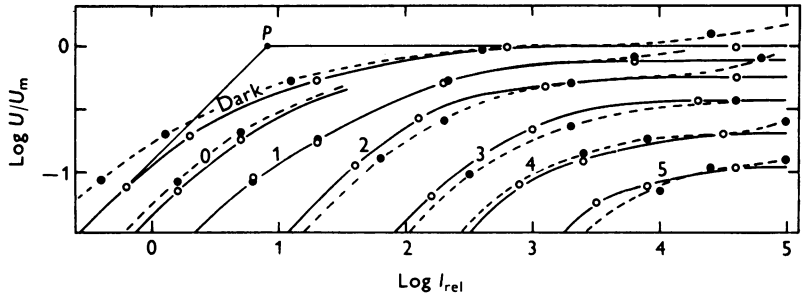


Fig. 4. Steady-state operating curves in darkness and with backgrounds log $I_{B\,rel}$ = 0–5. Flash stimuli: whole curves, open circles, log $I_{rel}$ = 0 corresponds to the bleaching rate $2 \times 10^{-8}$. $sec^{-1}$. Step of light stimuli: dashed lines, filled circles, log $I_{rel}$ = 0 corresponds to the bleaching rate $2 \times 10^{-10}$ $sec^{-1}$. Retina 11, 9° C.

An increase of the background intensity moves the curve predominantly to the right, as expected if the background decreases the transmitter coefficient $Q$. The minor downward movement is caused by the unavoidable transmitter background $c_1 = QI_B$.

In four retinae, the 40 msec flash responses $F$ and the step of light responses $S$ were compared. Threshold intensities were typically 2 log. units stronger for responses $F$ than for responses $S$, corresponding to an integrating time of the *on* response $\tau_1$ = 4 sec. Increasing the intensity $I_B$ moves both curves $F$ and $S$ approximately similarly to the right (see Fig. 4). Thus adaptation does not change the integrating time appreciably. This suggests that the main factor in the movement to the right is not a decrease of transmitter life time $\tau$ (assuming that $\tau$ is equal to $\tau_1$ or at least proportional to it). Therefore, the basic mechanism for the background adaptation in frog's rods appears to be the decrease of the transmitter release factor $q$. However, as seen in Fig. 4, the operating curve $S$ moves at first faster than the curve $F$. This tendency was also observed in other retinae, suggesting a small decrease also in the transmitter life time.

In Fig. 4 the responses $S$ start to increase again after saturation. This kind of secondary increase varied considerably but was usually quite small. It was probably caused by a cone contribution to the receptor potential.

In Fig. 5 the log relative thresholds log $I_t/I_0$ corresponding to a small criterion $U_c$ are plotted against the corresponding log $I_B$. The choice of the criterion is arbitrary as long as $U_c \ll U_{max}$. The curves drawn in Fig. 5 correspond to a generalized Weber function

$$I_t/I_0 = 1+(I_B/I_D)^\beta, \quad I_D = \text{constant}.$$

Weber's law holds for $\beta = 1$. All sets of the measured operating curves $F$ at 9 and 14° C gave $\beta$-values in the range 0·75–0·8. The exponent $\beta$ of curves $S$ is somewhat larger, because of the larger movement to the right of these curves.

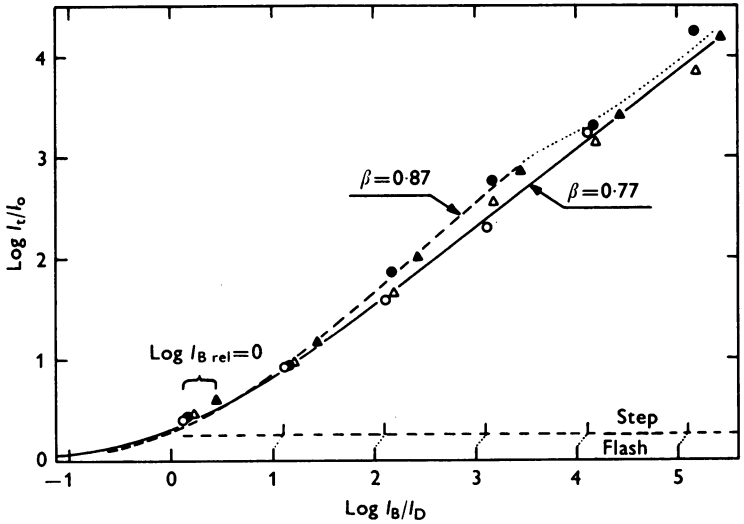


Fig. 5. Log. threshold *vs.* log. background intensity. The curves: $I_t/I_0 = 1+(I_B/I_D)^\beta$, $\beta$ = 0·77 for flash (continuous line, open symbols) and 0·87 for step stimulation (dashed line, filled symbols). Note slightly displaced scales for better fitting of the curves. The chosen $I_D$ values for each set of experimental points vary slightly: the first points of each set correspond to the same background, log $I_{B\,rel}$ = 0. Retina 9, circles; retina 11, triangles; 9° C.

Fig. 6 shows the steady-state paths of the crossing point in four retinae. Along each path the successive points correspond to tenfold increases of the background intensity. All paths indicate a strong movement to the right of the operating curve. Changes in the temperature do not affect the steady-state adaptation path of the crossing point noticeably. As expected according to Figs. 4 and 5, the path corresponding to the response $S$ extends somewhat more to the right than the path corresponding to the response $F$.

*Transients*

The movement of the operating curve during the *on* and *off* transients of the background light was determined using stimulating flashes at chosen times after onset or offset of the background. Thus the receptor potential recorded consisted of a superposition of the flash photoresponse on the background *on* or *off* response. Usually the flash response was easily separated because the background response was considerably slower. Sometimes the background response was recorded in isolation, so that it could be more accurately subtracted from the total potential. Instead of the whole operating curves merely the thresholds $I_t$ ($U_c$ = 12 $\mu$V) and the maximum responses $U_{max}$ were determined at chosen times during the transient.

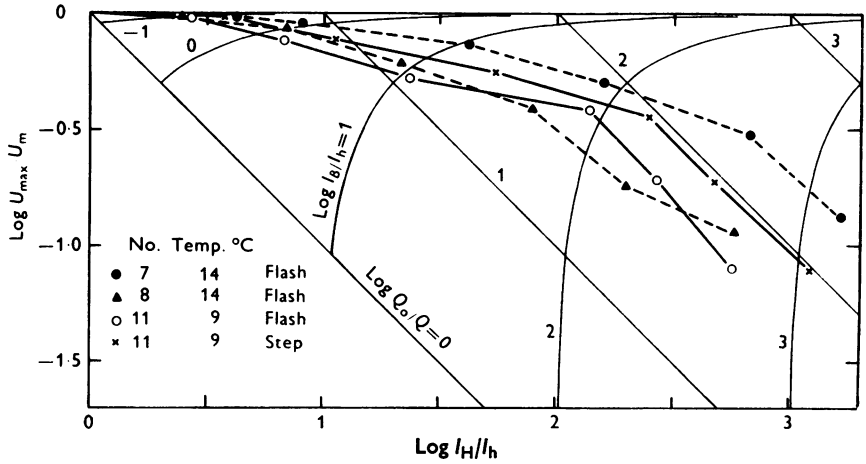


Fig. 6. Four stationary paths of the crossing point. The lines log $Q_o/Q$ = constant and the curves log $I_H/I_h$ = constant correspond to the model. Denoting $x$ = log $I_H/I_h$, $y$ = −log $U_{max}/U$ and $j_B$ = log $I_B/I_h$ the constant $Q$ lines are $y = x - \log Q_o/Q$ and the constant $I_B$ curves are $y$ = $-\log (1-10^{j_B-x})$. The six successive points along each path correspond to log $I_{B\,rel}$ = 0–5. Retinae 7, 8, and 11.

Fig. 7 shows the transients at three background intensities. The weakest background is log $I_{B\,rel}$ = 1, about fifteen-times the absolute threshold for the step of light. After an onset of the background both $I_t$ and $U_{max}$ reached their light-adapted values rapidly without any overshoot. After an offset $U_{max}$ returned to its dark-adapted value in *ca.* 30 sec. The log. threshold log. $I_t/I_0$ experienced during dark-adaptation a transient sensitization effect, 0·2 log. units, before returning to zero level. This kind of transient sensitization also occurred after few flashes of light used for

stimulation. Typically the threshold decreased *ca.* 0·3 log. units below absolute threshold and also $U_{max}$ increased little above $U_m$. This transient sensitization disappears in about 2 min.

At stronger backgrounds there occurs a large *threshold overshoot* during the *on* transient ('dazzling'). The threshold curve corresponding to log.

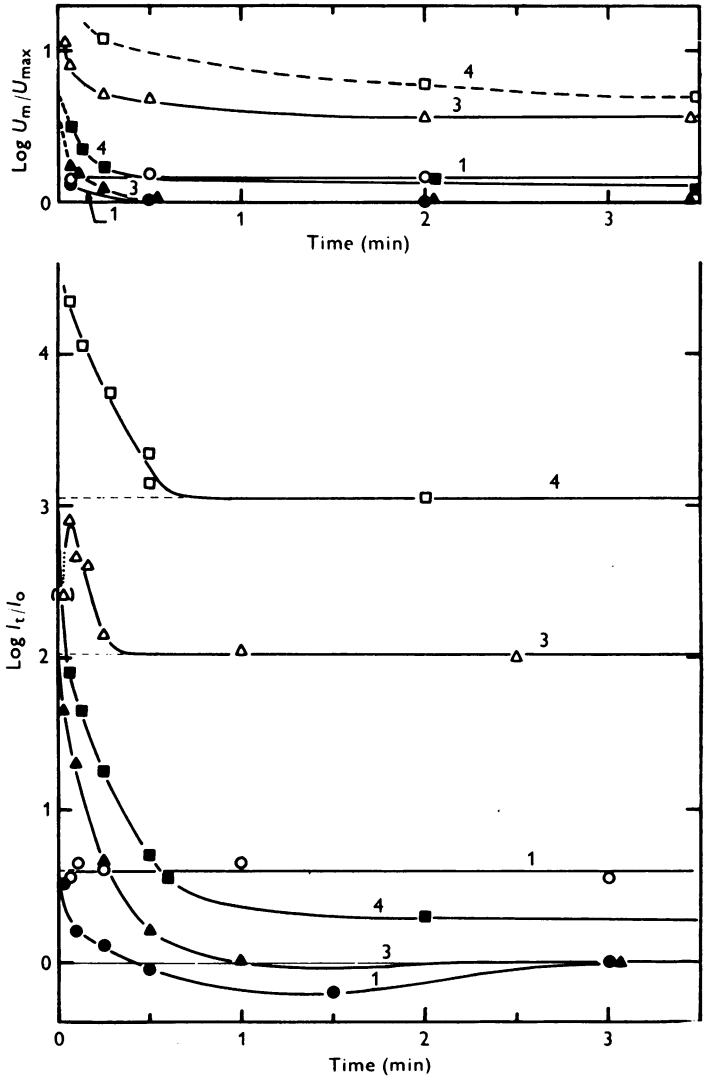


Fig. 7. The time courses of the log. threshold intensity and the log. amplitude during light-adaptation (open symbols) and dark-adaptation (filled symbols). Three background intensities: log $I_{B\,rel}$ = 1 (circles), 3 (triangles), and 4 (squares) indicated along the curves. Retina 8, 14° C.

TABLE 1. Magnitudes and half-times of adaptation transients

| Threshold transients | | | On | | Off | |
|---|---|---|---|---|---|---|
| Log $I_{B\,rel}$ | Temperature (°C) | Retina no. | $A$ | $t_{\frac{1}{2}}$ (sec) | $B$ | $t_{\frac{1}{2}}$ (sec) |
| 1 | 9 | 5 | 0·15 | 35 | 0·9 | 13 |
| | | 6 | 0·2 | 40 | 0·8 | 11 |
| | 14 | 7 | 0 | — | 0·7 | 4 |
| | | 8 | 0 | — | 0·6 | 4 |
| 3 | 9 | 5 | 1·4 | 16 | 2·2 | 20 |
| | | 6 | 1·3 | 17 | 2·3 | 12 |
| | 14 | 7 | 1·1 | 9 | 2·0 | 9 |
| | | 8 | 0·9 | 9 | 2·0 | 10 |
| | | 12 | 1·3 | 9 | 2·6 | 9 |
| 4 | 14 | 8 | 1·4 | 17 | 3·0 | 10 |
| **Amplitude transients** | | | **On** | | **Off** | |
| Log $I_{B\,rel}$ | Temperature (°C) | Retina no. | $C$ | $t_{\frac{1}{2}}$ (sec) | $D$ | $t_{\frac{1}{2}}$ (sec) |
| 1 | 9 | 6 | 0 | — | 0·15 | — |
| | 14 | 7 | 0 | — | 0·1 | — |
| | | 8 | 0 | — | 0·15 | — |
| 3 | 9 | 6 | 0·6 | 7 | 0·5 | 2 |
| | 14 | 7 | 0·4 | 6 | 0·5 | 5 |
| | | 8 | 0·5 | 7 | 0·55 | 4 |
| | | 12 | 0·7 | 15 | 0·75 | 2 |
| 4 | 14 | 8 | n.m. | n.m. | 0·7 | 8 |

The log. threshold *on* transient is $A = \log I_t^o/I_t^*$ and the *off* transient is $B = \log I_t^*/I_o$, where $I_t^*$ is the threshold in the light-adapted steady state and $I_t^o$ is the largest threshold observed during *on* transient (the maximum value at *ca.* 4 sec or the first measured value). Similarly, the log. amplitude *on* transient is $C = \log U^*_{max}/U^o_{max}$ and the *off* transient is $D = \log U_m/U^*_{max}$, where $U^*_{max}$ is the amplitude in the light-adapted steady state and $U^o_{max}$ is the first observed amplitude during *on* transient. The half-times ($t_{\frac{1}{2}}$) have been taken from the onset or from the offset of the background light to the time when half of the stated *logarithmic* transient is passed. (—) half-time could not be determined because the transient did not exist or was very weak; (n.m.) the transient was not measured.

$I_{B\,rel} = 3$ in Fig. 7 exhibits a maximum at $t \approx 4$ sec but the threshold values when $t \lesssim 4$ sec are uncertain because of the initial fast change of the background response. The *on* and *off* transients of the threshold intensity are about equally fast, the main processes being completed in about 30 sec at 14° C. Also the amplitude $U_{max}$ experiences 'dazzling', a transient overshoot of the $U_{max}$-compression after the onset of stronger

backgrounds. After both onset and offset of a strong background light there appears also small slower amplitude transients, lasting *ca.* 3 min.

These kinds of transient measurements were carried out in three retinae at 9° C and in three retinae at 14° C. The half-times and the magnitudes of the transients are presented in Table 1.

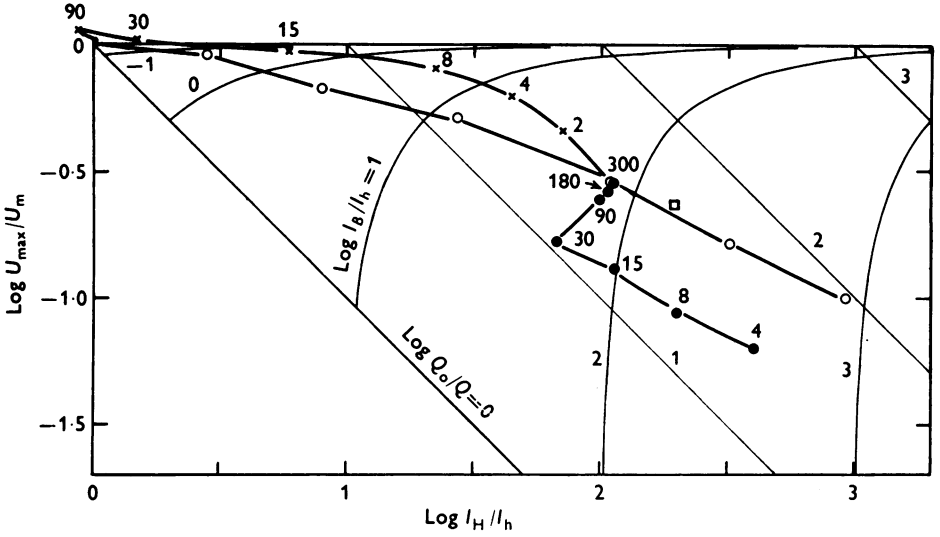


Fig. 8. A stationary path (○), a light-adaptation path (●), and a dark-adaptation path (×) of the crossing point. The numbers along the points indicate time in seconds after onset or offset of the background log $I_{B\,rel}$ = 3. Retina 12, 14° C. The open square indicates the rough position of the extrapolated stationary crossing point (log $I_{B\,rel}$ = 3) if the decrease of $Q$ were the only adaptation mechanism.

When $I_t$ and $U_{max}$ have been measured, the crossing point of the corresponding operating curve (the coordinate log $I_H/I_h$) can be calculated according to eqn. (7). The intensity corresponding to the abscissa of the crossing point is still denoted $I_H$, although it does not produce exactly the response $\frac{1}{2}U_{max}$ because the operating curve deviates from eqn. (3) (Michaelis equation).

Fig. 8 shows the paths of the crossing point during the *on* and *off* transients with the background log $I_{B\,rel}$ = 3, together with the steady-state path of that point when the background is varied. This is a typical path at this background level. When the background intensity is decreased, the measurable *on* transient (starting *ca.* 4 sec after onset of light) shortens and finally disappears. When the background intensity is

increased, the *on* transient becomes more pronounced and also the *off* transient path changes: because of the slow *off* transient of $U_{max}$ the *off* path follows more closely the steady-state path.

## DISCUSSION

When analysing the experimental results according to the model, it is first assumed that *the variation of the coefficient Q causes all the background adaptation effects*. The background intensity $I_B$ produces a transmitter concentration $QI_B$, while the step of light stimulus intensity $I$ produces the concentration $QI$. Substituting $c_1 = QI_B$ in eqns. (6) gives

$$I_H = c_0/Q + I_B \tag{8}$$
$$U_m/U_{max} = 1 + QI_B/c_0.$$

The constant-$Q$ lines and the constant-$I_B$ curves in Figs. 6 and 8 were calculated according to eqns. (3) and (8). At the background $I_B$ the crossing point should lie on the corresponding constant $I_B$ curve, the position along this curve being determined by the prevailing value of $Q$. When $I_B$ is increased tenfold, the crossing point of the stationary operating curve should jump from a constant-$I_B$ curve to another corresponding to a log. $I_B/I_h$ value 1 unit higher. As seen in Fig. 6 this is the case for small backgrounds $I_B \lesssim 100\ I_h$: the distance between the points along each path corresponds approximately to jumps from a constant-$I_B$ curve to the next.

The points of different paths clustered around the calculated curve $\log I_B/I_h = 0$ correspond to the background $\log I_{B\,rel} = 1$. The bleaching rate of that background was *ca.* $3 \times 10^{-9}$ sec$^{-1}$ (see Methods). A typical absolute threshold (criterion $U_c = 12\ \mu$V) corresponded to the bleaching rate $2 \times 10^{-10}$ sec$^{-1}$ and the typical maximum response was $U_m = 150\ \mu$V. Because $I_o/I_h = U_c/U_m$ the background $\log I_{B\,rel} = 1$ corresponds to

$$\log \frac{I_B}{I_h} = \log \frac{I_B/I_o}{U_m/U_c} \approx 0{\cdot}1.$$

This agrees with the value 0·0 of the calculated curve.

Above about $\log I_B/I_h = 2$ another adaptation process becomes noticeable: the jumps of the stationary crossing points are considerably smaller than predicted. This second adaptation process moves the operating curve predominantly to the left, indicating that the effect of the transient light is enhanced as compared to the steady light. The origin of this sensitization is discussed later. Note that the constant-$Q$ lines in Fig. 6 give underestimated $\log Q_o/Q$ values for the two last points of each path because those lines were calculated assuming the $Q$-decrease as a sole adaptation process.

When the background $I_B$ is turned on, the model predicts an immediate movement of the operating curve down along the 45° line, until the corresponding constant-$I_B$ curve is reached. This is the direct summation of $I$ and $I_B$. Then the decrease of $Q$ causes a movement along the constant-$I_B$ curve up to the stationary path. Apparently the $Q$-decrease is a fast process, because no large upward movement is seen in the *on* transient in Fig. 8 (the first recording was made 4 sec after onset of $I_B$). If the decrease of $Q$ were the sole adaptation mechanism, the stationary crossing point $\log I_{B\,rel} = 3$ would be roughly in the extrapolated position indicated by the square in Fig. 8. The first experimental values of the *on* transient are displaced somewhat *to the right* and *downwards*. The *on* transient is to the left (sensitization) in addition to the upward movement, resulting in *a stationary point on the left* of the expected position, as in the paths of Fig. 6.

When the background is turned off, the model predicts a displacement of the operating curve up along the 45° line. Then the increase of $Q$ should move the curve directly to the left. The *off* transient path of the crossing point in Fig. 8 agrees approximately with this prediction. However, after adaptation to a stronger background the *off* path follows roughly the stationary path, so that the return of the full amplitude is slower than expected.

Summarizing, the decrease of $Q$ as the main adaptation process explains most of the observed background adaptation results, on the presupposition that the decrease of $Q$ during the background *on* transient is quite fast. However, several features in the experimental results reveal further adaptation mechanisms especially at moderate or large background intensities. A minor *sensitivity-reducing process* leads to a displacement of the operating curve downwards and to the right, as seen few seconds after onset of the background (Fig. 8). The background onset also triggers a *sensitizing process*: the threshold to transient stimuli decreases considerably during the *on* transient (Figs. 7 and 8). As a result of this adaptation the stationary operating curves at strong backgrounds are displaced to the left (too small jumps of the stationary crossing point in Figs. 6 and 8). The *off* transient after extinguishing the background light is then a result of several processes. The temporary small hypersensitivity after offset of the background (Figs. 7 and 8) is probably a disappearing remainder of the sensitization. The slow recovery of the amplitude after an exposure to large background intensity may signify the decline of the sensitivity-reducing process.

The origin of the sensitization is possibly in the rod inner segment. The sensitization could be a manifestation of the transient increase of potassium permeability in the inner segment membrane induced by

hyperpolarization ('regenerative hyperpolarization': Brown & Pinto, 1974; Werblin, 1975). A decrease of sodium conductance in the hyperpolarized inner segment would be equally useful: it would compensate the effect of the observed decrease in the pumping rate (Sickel, 1973) and increase the sensitivity.

In addition to the decrease of $Q$ other possible adaptation processes in the rod *outer segment* were also included in the model. The increase of the plasma membrane parameter $G_L$ would move the operating curve predominantly down and somewhat to the left. The initial transmitter concentration $c_1$ could be larger than $QI_B$ because of some permanent transmitter background, moving the operating curve down along the 45° line. Neither of these processes is clearly discerned in the experimental results presented here. The minor extra sensitivity-reduction observed after onset of the background light could be an effect of these processes.

There are not much published data on background adaptation in the frog's rods that can easily be compared with the present results. Hood & Hock (1975) studied light-adaptation of the rod and cone receptor potentials in the aspartate-treated retinae of *Rana pipiens*. They measured thresholds using a 10 $\mu$V criterion response. The increase of threshold as a function of background intensity was similar to that reported here in Fig. 5. The observed saturation was probably caused by the decrease of amplitude towards the chosen criterion. The slope of the curve log $I_t$ *vs.* log $I_B$, stimulus 1 sec, was steeper than the slope corresponding to 50 msec stimulus, in agreement with the results of Fig. 5.

Background adaptation data on other species and on different receptor types reveal considerable quantitative differences. However, the decrease of $Q$ seems always to be the most important adaptation process. It is a general observation that the threshold follows roughly Weber's law in the range 2–6 decades. In several cases this dependence is clearly connected to the movement to the right of the operating curve: monkey cones (Boynton & Whitten, 1970), skate rods (Dowling & Ripps, 1972), gekko rods (Kleinschmidt, 1973), mudpuppy cones (Normann & Werblin, 1974). In mudpuppy rods the range of the $Q$-decrease may be unusually small, because the saturation appears without a clear range of Weber's law.

Alpern, Rushton & Torii (1970) claimed to have recorded operating curves of human rods by an ingenious indirect psychophysical method. The Michaelis equation was accurately fitted and Weber's law was that expected according to the model, including saturation. However, in disagreement with the general trend the operating curve moved directly down.

Time courses of the receptor hyperpolarization brought about by the background light have been recorded intracellularly in frog (Toyoda, Hashimoto, Anno & Tomita, 1970), in mudpuppy (Normann & Werblin,

1974) and in gekko (Kleinschmidt, 1973). The fast *on* transients in mudpuppy and gekko may indicate the decrease of $Q$, while the reported *on* transients in frog are slower, similar to the photoresponse transients reported here. In skate rod, a long-lasting insensitive period and a slow *on* transient are observed after background onset (Dowling & Ripps, 1972). Apparently the background first compress the amplitude below criterion (just detectable voltage, *ca.* 4 $\mu$V) and the decrease of $Q$ is exceptionally slow.

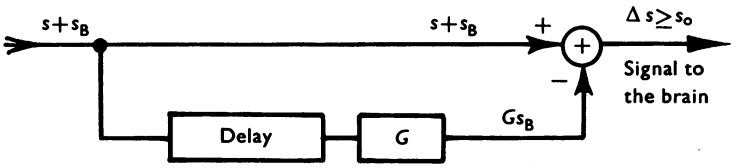


Fig. 9. A network adaptation scheme. The ganglion cell acts as a linear device summing the signals from the direct channel and the indirect channel. $s$, photoresponse to flash or step of light; $s_B$, receptor signal caused by a continuous background; $G$, relative gain; $\Delta s$, difference between signals received by two routes; $s_0$, absolute threshold signal of cell.

On the ganglion cell level the threshold–background relation is usually described quite accurately by Weber's law. In the frog this law holds well for 3·5 decades of background intensities when recorded from a ganglion cell (Donner, 1959; Donner & Reuter, 1968). Thus it is found that at least three mechanisms contribute Weber's law in the frog: the decrease of $Q$; the sensitization mechanism originating probably in the rod inner segment; and a network adaptation process which improves the threshold–background relation. It appears that Weber's law is a functional law, not a result of a specific physiological mechanism. The constant Weber-ratio is valuable for an animal: the contrasts on a given surface are independent of the illumination falling on that surface. Thus during evolution several suitable mechanisms have developed to bring about this law in co-operation. A simple signal-processing network demonstrates how receptor adaptation and network adaptation could co-operate. Let the receptor signals reach a ganglion cell through two channels. The direct channel is fast, the indirect channel has a delay but its gain is a little larger than the gain of the direct channel (relative gain $G$). The ganglion cell subtracts the signals of these channels and sends impulses to the brain if the difference exceeds the absolute threshold signal $s_0$ of that cell. Let $s_B$ be the receptor signal caused by a continuous background and $s$ be the photoresponse to flash or step of light. At the moment of the maximum response in the fast channel there is no signal $s$ in the indirect channel

yet. Thus the output of the ganglion cell is $s+s_B-Gs_B$. At the threshold $s = s_t$ this output just reaches the impulse-triggering value $s_o$. Therefore,

$$s_t/s_o = 1+s_B/s_D, \quad s_D = s_o/(G-1).$$

When $s_B \gg s_D$, Weber's ratio $s_t/s_B = s_o/s_D$ is obtained. All receptor adaptation processes included in the model decrease $s$ and $s_B$ in proportion, preserving the Weber's ratio. Thus a simple possibility for the co-operation of network and receptor adaptations is demonstrated. Otherwise the scheme is oversimplified, e.g. the receptive field of a ganglion cell varies depending on the state of adaptation (Donner & Reuter, 1965).

I am indebted to Professor K. O. Donner and Dr Tom Reuter for helpful discussions and criticism and to Ann-Christine Bäckström, Phil. lic., for valuable technical assistance. This work was supported by grants from the National Research Council for Sciences in Finland.

## REFERENCES

ALPERN, M., RUSHTON, W. A. H. & TORII, S. (1970). The attenuation of rod signals by backgrounds. *J. Physiol.* **206**, 209–227.

BAYLOR, D. A., HODGKIN, A. L. & LAMB, T. D. (1974). The electrical response of turtle cones to flashes and steps of light. *J. Physiol.* **242**, 685–727.

BOYNTON, R. M. & WHITTEN, D. N. (1970). Visual adaptation in monkey cones: recordings of late receptor potentials. *Science, N.Y.* **170**, 1423–1426.

BROWN, J. E. & PINTO, L. H. (1974). Ionic mechanism for the photoreceptor potential of the retina of *Bufo marinus*. *J. Physiol.* **236**, 575–591.

DONNER, K. O. (1959). The effect of a coloured adapting field on the spectral sensitivity of frog retinal elements. *J. Physiol.* **149**, 318–326.

DONNER, K. O. & HEMILÄ, S. (1975). Kinetics of long-lived rhodopsin photoproducts in the frog retina as a function of the amount bleached. *Vision Res.* **15**, 985–995.

DONNER, K. O. & REUTER, T. (1965). The dark-adaptation of single units in the frog's retina and its relation to the regeneration of rhodopsin. *Vision Res.* **5**, 615–632.

DONNER, K. O. & REUTER, T. (1968). Visual adaptation of the rhodopsin rods in the frog's retina. *J. Physiol.* **199**, 59–87.

DOWLING, J. E. & RIPPS, H. (1972). Adaptation in skate photoreceptors. *J. gen. Physiol.* **60**, 698–719.

FRANK, R. N. (1970). Electroretinographic response from the green rods of the isolated, perfused frog retina. *Vision Res.* **10**, 1101–1107.

FURUKAWA, T. & HANAWA, I. (1955). Effects of some common cations on electroretinogram of the toad. *Jap. J. Physiol.* **5**, 289–300.

HOOD, D. C. & HOCK, P. A. (1975). Light adaptation of the receptors: increment threshold functions for the frog's rods and cones. *Vision Res.* **15**, 545–553.

KLEINSCHMIDT, J. (1973). Adaptation properties of intracellularly recorded gekko photoreceptor potentials. In *Biochemistry and Physiology of Visual Pigments*, ed. LANGER, H., pp. 219–224. Berlin: Springer-Verlag.

MURAKAMI, M. & KANEKO, A. (1966). Differentiation of P III subcomponents in cold-blooded vertebrate retinas. *Vision Res.* **6**, 627–636.

NORMANN, R. A. & WERBLIN, F. S. (1974). Control of retinal sensitivity. I. Light and dark adaptation of vertebrate rods and cones. *J. gen. Physiol.* **63**, 37–61.

REUTER, T. & VIRTANEN, K. (1972). Border and colour coding in the retina of the frog. *Nature, Lond.* **239**, 260–263.

SICKEL, W. (1973). Energy in vertebrate photoreceptor function. In *Biochemistry and Physiology of Visual Pigments*, ed. LANGER, H., pp. 195–203. Berlin: Springer-Verlag.

SILLMAN, A. J., ITO, H. & TOMITA, T. (1969). Studies on the mass receptor potential of the isolated frog retina. I. General properties of the response. *Vision Res.* **9**, 1435–1442.

TOYODA, J., HASHIMOTO, H., ANNO, H. & TOMITA, T. (1970). The rod response in the frog as studied by intracellular recording. *Vision Res.* **10**, 1093–1100.

WERBLIN, F. S. (1975). Regenerative hyperpolarization in rods. *J. Physiol.* **244**, 53–81.